



THE UNIVERSITY *of* EDINBURGH

Edinburgh Research Explorer

Collapse-resisting mechanisms of planar trusses following sudden member loss

Citation for published version:

Yan, S, Zhao, X & Lu, Y 2017, 'Collapse-resisting mechanisms of planar trusses following sudden member loss' *Journal of Structural Engineering*, vol. 143, no. 9, 04017114. DOI: 10.1061/(ASCE)ST.1943-541X.0001849

Digital Object Identifier (DOI):

[10.1061/\(ASCE\)ST.1943-541X.0001849](https://doi.org/10.1061/(ASCE)ST.1943-541X.0001849)

Link:

[Link to publication record in Edinburgh Research Explorer](#)

Document Version:

Peer reviewed version

Published In:

Journal of Structural Engineering

General rights

Copyright for the publications made accessible via the Edinburgh Research Explorer is retained by the author(s) and / or other copyright owners and it is a condition of accessing these publications that users recognise and abide by the legal requirements associated with these rights.

Take down policy

The University of Edinburgh has made every reasonable effort to ensure that Edinburgh Research Explorer content complies with UK legislation. If you believe that the public display of this file breaches copyright please contact openaccess@ed.ac.uk providing details, and we will remove access to the work immediately and investigate your claim.



Collapse-resisting mechanisms of planar trusses following sudden member loss

Shen Yan¹, Xianzhong Zhao², Yong Lu³

1. Ph.D., College of Civil Engineering, Tongji Univ., Shanghai 200092, China; College of Aerospace Engineering and Applied Mechanics, Tongji Univ., Shanghai 200092, China. E-mail: s.yan@tongji.edu.cn

2. Professor, College of Civil Engineering, Tongji Univ., Shanghai 200092, China; State Key Laboratory of Disaster Reduction in Civil Engineering, Tongji Univ., Shanghai 200092, China (corresponding author). E-mail: x.zhao@tongji.edu.cn

3. Professor, Institute for Infrastructure and Environment, School of Engineering, the Univ. of Edinburgh, Edinburgh EH9 3JL, UK. E-mail: yong.lu@ed.ac.uk

Abstract:

Progressive collapse incidents of truss structures are often reported; however, studies on the collapse resistance of truss structures are comparatively few. In order to investigate the collapse-resisting mechanisms of truss structures, this paper presents a comprehensive and detailed study on the collapse-resisting performance of planar trusses subjected to local damage at various locations, using both finite-element (FE) and analytical approaches. An improved FE analysis procedure is proposed to improve the computational efficiency. The main conclusions include: (1) in the case of a sudden loss of a top chord member or a diagonal member, catenary action will be the primary mechanism to provide the bridging-over capacity of the remaining structure, and severer damage can be resulted when the removed member locates in the mid-span; (2) if a bottom chord member is suddenly lost, arch action will be the main mechanism to provide the bridging-over capacity of the remaining structure, and severer damage can be resulted when the removed member locates next to the support or in the mid-span.

24 Keywords:

25 planar truss; progressive collapse; collapse-resisting mechanism; finite element analysis; critical members

26 **Introduction**

27 Structures may encounter unexpected local failures caused by human errors or natural hazards during their long-time
28 service, and as a result a progressive collapse may be triggered in a chain reaction. Since the collapse of the World Trade
29 Center towers in 2001 (NIST 2005), extensive studies, by means of experimental approaches (Yi et al. 2008; Sasani and
30 Sagioglu 2008; Chen et al. 2011; Song et al. 2014) and numerical studies (Luccioni et al. 2004; Khandelwal et al. 2009;
31 Fu 2009; Fang et al. 2011), have been conducted to investigate the progressive collapse resistance of framed building
32 structures.

33 However, studies on the collapse-resisting performances of truss structures widely used in large-span roofing systems
34 and bridges are comparatively few. Reports on progressive collapse incidents of truss structures clearly suggest that this
35 situation needs to be improved. In 1978, the space truss roof of the Hartford Civic Center collapsed after a snowstorm
36 (Smith and Epstein 1980); the buckling of a few compressive top grid members was deemed to be the immediate cause of
37 the total collapse. In 1979, the south side roof of the Kansas Kemper Arena collapsed in the strong winds and heavy rains
38 (Levy and Galvadori 1992); the collapse was believed to be induced by the failure of a few bolts. Progressive collapse
39 incidents of steel truss bridges have also been reported. The I-35W Bridge over the Mississippi River in Minneapolis
40 suddenly collapsed in 2007 with 13 people killed and 145 others injured (NTSB 2008; Astaneh-Asl 2008); the primary
41 cause was the fracture of local undersized gusset plates under increased dead load from repair and reinforcement of the
42 slab over years.

43 Studies on the progressive collapse resistance of truss structures available in the literature used mainly numerical
44 approaches, in which a load-bearing element was removed to evaluate the general integrity of the structures and their
45 capacities in redistributing the loads. Murtha-Smith (1998), Malla and Nalluri (2000) and Jiang and Chen (2012) showed
46 that although truss structures had a large degree of redundancy, progressive collapse could occur following the potential
47 loss of a single critical member. Miyachi et al. (2012) investigated the progressive collapse processes of steel truss bridge

48 models with different span ratios under four live load cases. Zhao et al. (2016) conducted a series of benchmark progressive
49 collapse tests on planar Warren trusses by suddenly removing one of the diagonal members; in these tests, the influences
50 of joint stiffness on the collapse resistance were studied. The collapse-resisting mechanism of structures following a
51 member loss has been studied by many researchers, most of them focused on frame structures. Two main resistance
52 mechanisms for frame structures against progressive collapse have been identified: a) the catenary action developed in the
53 beams right above a removed middle column (Yi et al. 2008; Sasani and Kropelnicki 2008). Before the catenary action is
54 fully developed, a certain degree of arch action may be formed in the beams as a transitional mechanism, which resulted
55 from the shifting of the neutral axis in the beam cross-section caused by either cracking in RC beam case (Yi et al. 2008)
56 or the elevated center of rotation in steel connections (Izzuddin 2005). b) the Vierendeel (frame) action for the redistribution
57 of the loads when a corner column is removed (Sasani and Sagiroglu 2008). With regard to truss structures, Zhao et al.
58 (2016) demonstrated the contribution of catenary action in the bottom chord under a diagonal member loss scenario.
59 However, the collapse-resisting mechanisms and associated structural responses may not be the same and have not been
60 addressed for loss of a member other than the specific diagonal member considered in their test program.

61 Another important issue that needs to be addressed is how to identify the critical members, which in the context of
62 progressive collapse is defined as the members whose removal cause the most severe damage. Identifying critical members
63 helps reduce the computational cost when collapse-resistance designs are conducted on structures with many structural
64 members. According to current codes and guidelines for progressive collapse design of frame structures (GSA 2003; DoD
65 2009), columns located at or near the middle of both the short side and the long side of a building, as well as those at
66 corners are considered critical. The collapse-resistance analysis thus can be conducted by removing these members one at
67 a time. However, there is no such codified recommendation for large-span structures including truss structures yet.

68 In this paper an extensive finite-element (FE) analysis is performed to study the response of planar trusses to a sudden
69 member loss at various key locations. The analysis employs a modelling procedure which contains several integral steps

70 and is put forward to improve the overall analysis efficiency as well as the accuracy. The modeling strategy is first validated
71 through comparisons with results of the previously mentioned tests by Zhao et al. (2016). Based on the FE analysis results,
72 the potential mechanisms for resisting and redistributing loads in planar trusses are examined. A detailed study on these
73 mechanisms using both simplified analytical and FE approaches is carried out and critical members are identified.

74 **Finite element model and validation**

75 *An improved FE analysis procedure*

76 Numerical analysis methods with varying complexities, including for example the dynamic effect and geometric and
77 material nonlinearities, may be used to study the response of structures following the loss of members. The potential
78 advantages and shortcomings of several analysis procedures have been discussed by various researchers (Marjanishvili
79 2004; Powell 2005; Marjanishvili and Agnew 2006; Tsai and Lin 2008). Generally speaking, a static analysis using existing
80 code guidelines (GSA 2003; DoD 2009) may be over-conservative (Powell 2005). When more precise results are desired,
81 a nonlinear dynamic analysis would be required. Hence, the nonlinear dynamic analysis approach is adopted in this study.

82 When nonlinear dynamic analysis is performed, the static initial condition, including the statically balanced
83 configuration under static loading and the associated stress/strain field, should be well established before the member
84 removal. In a progressive collapse scenario, local damage usually occurs in a very short time, and this also causes transient
85 dynamic effects. Therefore, it is preferable to employ an explicit time integration scheme in which the time-increment is
86 dictated by the convergence requirement of the conditionally convergent explicit algorithms, and hence is sufficiently small
87 for the transient dynamic analysis. Moreover, use of the explicit solver allows for element deletion that is not possible in
88 an implicit solver due to force equilibrium convergence requirements. This gives the explicit solver another advantage for
89 the progressive collapse analysis because structural members may break during collapse and consequently need to be
90 deleted from the structural model. However, if the same explicit scheme is employed to obtain the statically balanced state
91 under external loads including gravity, the loads need to be applied on the FE model very slowly to exclude unwanted

92 kinetic energy, thus making the analysis computationally expensive. In order to effectively perform a progressive collapse
93 analysis in commercial FE packages such as ABAQUS (ABAQUS Inc. 2010), it would be desirable to run an implicit time
94 integration (ABAQUS/Standard) analysis first to establish the initial static balanced state. The deformed mesh of the
95 structural model and its associated material state is then imported into an ABAQUS/Explicit solver to carry out the dynamic
96 progressive collapse analysis. To realize the removal of a structural member in this explicit time integration analysis, the
97 structural model is modified such that the particular structural member is physically removed from the mesh but the original
98 internal forces of this member are retained. These internal forces are then deactivated to trigger the progressive collapse of
99 the structural model. A similar operation procedure may be employed when using some other explicit time integration FE
100 packages, such as LS-DYNA (Hallquist 2007).

101 Such a FE analysis procedure requiring a restart can be laborious because many manual operations are involved. To
102 tackle this problem, an improved procedure for the implementation of structural progressive collapse analysis in an explicit
103 scheme (ABAQUS/Explicit in particular) is provided herein. This procedure is divided into three steps, and by employing
104 specially designed user subroutines it eliminates the needs of a restart analysis and manual operations, thus the analysis
105 can be performed continuously and efficiently.

106 The first step is called the pseudo-static loading step. In this step, after applying the gravity and other external loads on
107 the structural model in a sufficiently short time period, viscous damping forces are applied on model joints through
108 ABAQUS/Explicit user subroutine VUMAP (ABAQUS Inc. 2010) to damp out the structural vibration and achieve a
109 statically balanced state with a minimal number of time increments. At each joint, VUMAP defines the dependence of
110 applied viscous damping force F_v on the real-time velocity of this joint v ; v is obtained through ABAQUS/Explicit utility
111 routines vGetSensorValue (ABAQUS Inc. 2010). Both linear and nonlinear dependences can be specified; in this study,
112 moderate damping force is applied by specifying square root dependence, as shown in Eq. 1.

113
$$F_v = \text{sign}(v) \times c_v \times \sqrt{|v|} \quad (1)$$

114 where, c_v is the user-defined viscous parameter, which is related to the external load and the stiffness of the structure and
115 thus is difficult to be explicitly calculated. Several tentative analyses of the first step may be needed in order to determine
116 an appropriate value of c_v , to ensure that the kinetic energy at the end of the first step is sufficiently small.

117 The second step is called the element removal step, during which a user subroutine VUSDFLD (ABAQUS Inc. 2010)
118 is adopted to conveniently delete the target member from the mesh in a pre-defined fashion. In VUSDFLD, a field variable
119 (FV) is used to simulate the stiffness reduction characteristic of the member during its removal, and a state-dependent
120 variable (SDV) is used to delete the elements of this member. Stiffness reduction is realized by reducing the Young's
121 Modulus of the removed member, which is defined to be dependent on FV (an example of the dependence is shown in Fig.
122 1a) and thus can be changed in different steps by manipulating FV, as shown in Fig. 1b. After the Young's Modulus is
123 reduced to a very small value (Young's Modulus cannot be zero in ABAQUS), the element can be further deleted from the
124 model by setting SDV from one to zero (By the default rules of ABAQUS/Explicit, if SDV value of an element equals to
125 one, the element is active, while a value of zero indicates that ABAQUS/Explicit deletes the element from the model by
126 setting the stresses to zero).

127 The third step is called the dynamic response step, during which the response of the remaining structure following the
128 member removal is calculated through explicit time integration scheme in ABAQUS/Explicit.

129 A simple two-dimensional problem is employed here to demonstrate this improved FE analysis procedure for a
130 progressive collapse analysis. As shown in Fig. 2, two weightless pinned-end bars (A and B) are connected at the bottom
131 where an object with a unit weight is attached. Bar A breaks suddenly in 0.1 s, and the response of bar B (including its
132 axial force and the bottom end displacement) is to be studied.

133 In the FE model, each bar is modeled with a two-node linear planar beam element in ABAQUS/Explicit (element B21),
134 and a point mass with unit weight is applied at the bottom. The whole time period of the analysis is 5 s, with 0.2 s, 0.1 s
135 and 4.7 s for the three individual steps, respectively. In the last 0.2 s of the third step, a horizontal viscous force is applied

136 on the bottom end of bar B, through the user subroutine VUMAP, to save computing time in obtaining the final balanced
137 state. Fig. 3 presents the FE results, which agree well with the expectation that bar B moves like a swinging pendulum and
138 finally gets settled at the vertical position (see Fig. 2). Neither restart nor other manual operations are required for the entire
139 analysis procedure, and importantly, the establishment of the statically balanced state under static load can be achieved
140 only in 0.2 s, which significantly increases the computationally efficiency.

141 *FE modeling strategy of trusses and benchmark experimental truss structures*

142 The proposed FE modelling strategy for trusses is first implemented on the experimental truss structures as reported in
143 Zhao et al. (2016) for verification and validation purposes. Fig. 4 presents an overview of the test program. Three Warren
144 truss specimens carrying gravity loads were tested under a sudden member removal scenario. It was found that the truss
145 with welded joints (truss-WJ) and the truss with pinned joints between diagonal members and the continuous chords (truss-
146 PJ) regained a balanced state without severe damage, but the truss in which the diagonal members were connected to the
147 continuous chords through rigid joints (truss-RJ) collapsed due to successive buckling of several other diagonal members.

148 FE models of truss-PJ and truss-RJ are developed in ABAQUS/Explicit, and the analysis strategy presented above is
149 implemented. A schematic of the models is shown in Fig. 5. The truss members are modeled with two-node linear space
150 beam elements (Element type B31 in ABAQUS) with a pipe cross-section, and the material is modeled using a piecewise-
151 linear plasticity model, with stress-strain curves based on coupon test data. The joint connectors are modeled with B31
152 elements with a rectangular cross-section and a circular cross-section, while an elastic material model is adopted. The
153 difference between these two truss models for simulating the two test specimens lies in the connecting method between the
154 diagonal members and the joint connectors. As shown in Fig. 5, a rigid connection is adopted in the truss-RJ model, while
155 the in-plane rotational degree of freedom is released in the truss-PJ model. The point loads, which were applied at top chord
156 joints by means of hanging iron plates in the tests (see Fig. 4b), are modeled with lumped masses. Boundary conditions are
157 defined in order to be consistent with the tests, such that the two edge supports are free to rotate in-plane, but the vertical

158 and horizontal translational degrees of freedom are restrained; at all the top and bottom chord joints, where the lateral out-
159 of-plane deformation was not allowed by a pair of plexiglass plates in the tests (see Fig. 4b), the out-of-plane translational
160 and rotational degrees of freedom are also fully restrained. Meanwhile, a hard contact between the joint connectors and the
161 opposite chord members is specified, to simulate the fact that the joint connectors were not allowed to pass through the
162 chord members in the tests.

163 Attention should be paid to the material damping when dynamic FE analysis is performed. According to a previous
164 study (Wang 2010), different structural responses can be observed in a progressive collapse analysis when the viscous
165 damping varies. Hence, the damping property of the tested trusses should be realistically determined and included in the
166 FE model. Rayleigh damping is one of the most commonly used types of viscous damping. Since the primary dynamic
167 response after a sudden loss of a member is governed by the lowest mode, using a mass or stiffness proportional damping
168 would not make a significant difference. Considering the computational efficiency, however, a mass proportional viscous
169 damping is preferred in an explicit time integration analysis since the stiffness proportional viscous damping would require
170 a significantly smaller stable time increment of the analysis (Abaqus Inc. 2010), meaning a reduced the computational
171 efficiency. The accurate value of the mass proportional viscous damping factor α varies with the circular frequency ω that
172 is related to the structural configuration and thus changes during collapse. In this study, ω of the final balanced
173 configuration was chosen as the reference, which was about 32 rad/s according to the truss tests (natural frequency was 0.2
174 s). Free vibration measurements from the tested trusses under this configuration suggested that the damping ratio ζ was
175 about 3%. This value is consistent with the commonly used damping ratio of space steel structures. Hence, α is calculated
176 to be 2.0.

177 The analysis has been run following the improved FE analysis procedure. In the first step, the gravity load was applied
178 in 0.1 s, then the vertical viscous damping forces were applied at all the top chord joints for another 0.1 s. In the second
179 step, the target elements (DM2, see Fig. 4a) was deleted within 0.06 s, where the reduction curve of the Young's Modulus

180 was carefully defined, as shown in Fig. 1b, to ensure good replication of the axial force reduction characteristic of DM2 in
181 the tests. The third step lasted for 2.0 s, during which the response of the remaining structure was calculated.

182 *FE results and validation*

183 Fig. 6 shows the response of FE model of truss-PJ during the first step analysis. As can be seen, the kinetic energy of the
184 whole model reduced to zero quickly after the application of the vertical viscous damping forces, and the vertical
185 displacement at the mid-span stabilized at -3.35 mm which correlated well with the vertical displacement calculated by
186 implicit analysis (ABAQUS/Standard). Hence, the scheme is deemed to be effective and the static balance of the truss-PJ
187 model is achieved at the end of the first step analysis (in 0.2s). Fig. 7 presents the comparison between the FE results and
188 the experimental measurements of the average axial strain of the removed member DM2. It can be observed that the
189 removal of DM2 was well simulated in the FE analysis. This confirms that the proposed FE analysis procedure, which has
190 been demonstrated in the previous two-bar model, works effectively also in the progressive collapse analysis of planar truss
191 structures. It is noted that to facilitate comparisons between the FE and test results, the beginning of the second step, i.e.
192 when the removal of elements started, is taken as time = 0.0 second so that the timescale in the FE analysis is consistent
193 with the experimental results.

194 The FE model of truss-PJ regains a balance after the removal of member DM2, which is in good agreement with the
195 test observation. Fig. 8 presents the comparisons between the FE predictions and the experimental measurements of several
196 important structural responses, including the vertical displacement of BJ1 and the strain responses in TC1 and BC1 (“+”
197 and “-” in the legend represents strain on the top and bottom surface of the member, respectively). It is noted that in the
198 tested trusses these responses were closely related to the load-redistributing mechanism, therefore, the good agreement
199 observed between the FE and the experimental results indicates that the FE analysis is capable of capturing the key
200 structural response when truss structures are subjected to a member loss.

201 For truss-RJ which experienced progressive collapse after the member removal, Table 1 shows the comparisons of

202 corresponding time instances of key collapsing stages between the FE predictions and the experimental measurements. It
203 can be seen that the sequence of member failure is well predicted by the FE model. Except for a 0.19 s difference for the
204 time when TJ2 dropped onto the bottom chord, all other time instances match very well with the test results. Good
205 agreement is also observed at the strain level, as shown in Fig. 9, which again confirms the efficiency and accuracy of the
206 current FE analysis procedure.

207 **Influence of varying member removal locations**

208 Having verified the FE model and the analysis procedure, in this section we examine the influence of varying member
209 removal scenarios and the associated collapse mechanisms. According to the aforementioned benchmark experiments, the
210 pin-jointed truss-PJ behaved similarly to the welded-joint truss under a collapse scenario; therefore, the FE model of truss-
211 PJ is adopted as the reference case for the parametric study to represent both pinned and welded joint cases. The external
212 load applied onto the FE model is kept the same as that considered in the experimental program.

213 Fig. 10 shows the deformed structure after a local failure (removal) occurred at a top chord member, herein member
214 TC2. The remaining structure regains a balance through the catenary action developed along the bottom chord, and this
215 can be characterized by a considerable overall vertical deflection and large tensile strain in the bottom chord.

216 A simplified analysis can be performed to explain the development of the catenary action in such a top-chord removal
217 scenario, as shown in Fig. 10a. Upon the removal of the top chord member, the sub-structures on both sides of the local
218 damage are still composed of stable triangular grids and thus can be considered as intact parts. These two sub-structures
219 are effectively joined by a “connection”, which in the case here is formed by the bottom chord joint right below the removed
220 member, and consequently an alternate load-transferring path through this connection to the supports is formed. Because
221 the vertical stiffness of this alternate load-transferring path, which is dictated by the bending stiffness of the horizontal
222 bottom chord, is very limited, the remaining structure would not be capable of maintaining a static balance under the
223 original configuration, and thus a large deflection becomes inevitable. As a result, catenary action develops in the tilted

224 bottom chord, and the vertical component of this action provides the vertical resistance and stiffness required to carry the
225 external load. In summary, catenary action arises from the need of sufficient vertical stiffness to maintain or regain the
226 bridging-over capacity after local damage. For a local failure occurring at any other top chord member, a similar
227 deformation pattern and collapse-resisting mechanism can be anticipated.

228 The above conceptual analysis involving a “support–connection–support” path can also be applied to the response
229 prediction of trusses subjected to bottom chord member loss. Take the removal of member BC3 as an example, as shown
230 in Fig. 11 a, the alternate load-transferring path becomes a three-hinged arch with top chord joint TJ3 being the “connection”.
231 Such an arch effect has considerable vertical stiffness, and so the remaining structure could bridge over the local damage
232 under the original geometric configuration. This mechanism is referred to herein as the “arch action” in a damaged truss.
233 The formation of an arch action can also be confirmed through strain readings; both the upper chord and the bottom chord
234 are under compression after the removal of the bottom chord member, as shown in Fig. 11b.

235 When local damage occurs in a diagonal member, such as DM5 shown in Fig. 12a, the undamaged sub-structures will
236 tend to be joined by two “connections”, through the top chord member above the removed diagonal member (TC2 herein)
237 and the bottom chord member below the removed diagonal member (BC3 herein), respectively. Hence, there are two
238 potential alternate load-transferring paths. Arch action could be developed in the top alternate load-transferring path in the
239 original geometric configuration, but the load resistance however can be very limited because the top connection here
240 depends on a slender member (TC2), which will tend to buckle under a large compressive force. Moreover, if the removed
241 diagonal member is not near the mid-span, different external loads on the two undamaged sub-structures can generate large
242 shear force in the top connection (a top chord member), which increases the buckling risk. Therefore, as shown in Fig. 12,
243 when the load-transferring path under the above arch action is interrupted, catenary action can subsequently develop in the
244 bottom alternate load-transferring path. To sum up, considering the unstable nature of the arch action due to the buckling
245 potential of the compressive top connection, the catenary action developed in the bottom chord is regarded as the major

246 collapse-resisting mechanism when a local failure occurs in a diagonal member.

247 Warren truss has been the main structural type considered in our experimental study. For other types of truss structures,
248 such as the modified Warren truss and the Pratt truss, there are vertical members in addition to diagonal members. A FE
249 model of a modified Warren truss has been developed on the basis of truss-PJ model, as shown in Fig. 13. Vertical members
250 are added at all bottom chord joints, and the external load is reassigned to all top chord joints (the number of the top chord
251 joints is increased from 5 to 9). The numerical results demonstrate that when subjected to the loss of a chord member, the
252 modified Warren truss also exhibits a typical “support–connection–support” alternate load-transferring path, similar to the
253 case of the Warren truss. Moreover, the progressive collapse resistance under such chord-member removal scenarios does
254 not seem to increase by the presence of the vertical members. This is because when a top chord member is removed, the
255 vertical members do not contribute to the development of the catenary action in the bottom chord; and when a bottom chord
256 member is removed, although the stiffness and the strength of the two undamaged sub-structures (parts of the compressive
257 arch) is enhanced to some extent by the vertical members, there is limited beneficial effect for the load resistance of the
258 arch action because the internal force of the diagonal member and the bottom chord member next to the truss support is
259 not changed. It is noted here that in a later analysis, the load resistance of the arch action in a truss with a bottom-chord
260 loss is found to be determined by the loading conditions of these two members.

261 When the modified Warren truss is subjected to the loss of a diagonal member, however, different responses are
262 observed as compared with the Warren truss. Because the unbraced lengths of the compressive top chord members are
263 reduced by half due to the presence of the vertical members, and thus the buckling potential of the connection of the top
264 alternate load-transferring path is reduced. As a result, the arch action is maintained after DW5 is removed, and the catenary
265 action in the bottom alternate load-transferring path is not ‘triggered’. When the modified Warren truss is subjected to the
266 loss of a vertical member itself, the overall strength and stiffness of the truss is not significantly reduced. At this time, the
267 two triangular grids merge into one stable triangular gird, as shown in Fig. 14, and thus the remaining structure can regain

268 balance easily with very low risk of developing into a progressive collapse.

269 **Collapse-resistance mechanisms in trusses**

270 *Catenary action*

271 According to the previous discussion, catenary action in the bottom chord provides the bridging-over capacity when initial
272 damage occurs at a top chord member or a diagonal member. As observed in the experiment of truss-WJ mentioned above,
273 the catenary action helped the damage structure to regain balance under an equivalent distributed roof load of 1.59 kPa,
274 indicating that the load resistance of such a catenary action is remarkable. However, utilization of the catenary action must
275 be subjected to certain restriction, and in particular the vertical deflection of the remaining structure should not be too large.
276 There are two reasons. On the one hand, a large vertical deflection implies a risk to cause casualties underneath the truss
277 structure, and this could mean effectively a collapse state of the truss although there is no code provision specifying such
278 a deflection limit currently. On the other hand, a large deflection would lead to a large rotation at the bottom chord joint
279 which forms the critical “connection” of the undamaged sub-structures (see Fig. 10a). This would result in large bending
280 moments at the ends of the web members and thus increase the risk of web-member buckling and the progressive collapse
281 of the remaining structure. Therefore, vertical deflection should be restricted when catenary action provides the major
282 collapse resistance of a truss structure.

283 Fig. 15 presents the simplified analytical model reflecting the catenary action developed over the bottom chord of
284 trusses. The model enables the study of the distribution of the critical top chord members. If the local damage occurs at a
285 distance of pL from the left truss support (L is the span of the truss and p varies from 0 to 1), the distributed external vertical
286 load q under a force equilibrium condition can be expressed in terms of L , p , the ratio of vertical deflection Δ to span L ,
287 and the tensile force in the catenary member (bottom chord) T , as given by Eq. 2.

$$288 \quad q = \frac{2}{L} \cdot \frac{\Delta}{L} \cdot \frac{1}{p(1-p)} \cdot T \quad (2)$$

289 For a certain deflection limit value of Δ/L (which may be determined from relevant code provisions), the load resistance

290 q provided by the catenary action can be determined by p and T . Due to the material nonlinearity characteristic of the
 291 bottom chord, T is difficult to calculate. However, it can be understood that T is positively correlated to the elongation of
 292 the catenary member δL , as expressed in Eq.3. The elongation δL can in turn be approximately calculated by p and Δ/L
 293 based on the geometric calculation of the deformed bottom chord, as expressed by Eq. 4.

$$294 \quad T \propto \delta L \quad (3)$$

$$295 \quad \delta L = \left(\sqrt{p^2 + \left(\frac{\Delta}{L}\right)^2} + \sqrt{(1-p)^2 + \left(\frac{\Delta}{L}\right)^2} - 1 \right) \cdot L \quad (4)$$

296 Therefore, for a given Δ/L limit, T depends on p and as a result the load resistance q of the catenary action depends on
 297 p only. In Fig. 16, the term of $1/p(1-p)$ and δL is plotted against p (deflection limit Δ/L is set as 1/5 for an example). It is
 298 observed that smaller values of $1/p(1-p)$ and δL are obtained when p approaches 0.5. Consequently, according to Eq. 2 and
 299 Eq. 3, when the local damage of a top chord or a diagonal member is near the mid-span, the load resistance q provided by
 300 the catenary action is the smallest. In other words, when the catenary action provides the major collapse resistance, the
 301 critical members are the top chord and the diagonal member near the mid-span of the truss.

302 The above argument is verified using FE analysis, but truss-PJ may not provide sufficient generality because there are
 303 only two top chord members on each side of the axis of symmetry. Therefore, a further FE model referred to as truss-PJ-
 304 LS (LS denotes long span) is set up to include more top chord members, as shown in Fig. 17. The grid size, member cross-
 305 sections and the material properties of the new model remain the same as that of truss-PJ, but the span is doubled.
 306 Considering the bending moment in the mid-span of a truss increases with the square of the truss span, the external
 307 distributed load on truss-PJ-LS, which is also applied as point loads on all top chord joints, is reduced to one fourth of that
 308 applied on truss-PJ, so that the same mid-span bending moment is retained.

309 The FE results from truss-PJ-LS show that when subjected to the loss of any one of the top chord members, the catenary
 310 action developed in the bottom chord provides collapse resistance. As shown in Fig. 18 for a typical case, the balanced
 311 configurations are entirely consistent with the predictions based on the alternate load-transferring path with the “support–

312 connection–support” assumption.

313 Fig. 19a presents the largest vertical displacements, which occurs at the bottom chord joint right below the removed
314 top chord, under different top-chord removal scenarios. It can be observed that the final stabilized vertical displacement
315 increased when the removed top chord is closer to the mid-span of the truss, and the increase trend becomes smooth when
316 the removed top chord approaches the mid-span. This is consistent with the trend expressed in Eq. 2~ Eq. 3 and Fig. 16.
317 Moreover, it is also observed that among all the bottom chord members, the one in the middle of the sub-structure with a
318 longer span has evidently larger tensile strain than that of the other bottom chord members. Note that when one of the top
319 chord member at the left part of the truss is removed, the right-hand side sub-structure has a longer span; conversely, the
320 left-hand side sub-structure has a longer span. Based on the fact that the middle bottom chord member of a typical intact
321 truss has the largest tensile force, the sub-structures on both sides of the local damage may be deemed as undamaged truss,
322 therefore, the “support–connection–support” assumption is confirmed.

323 Fig. 19b presents the strain responses of the bottom chord members with the largest tensile force under different top-
324 chord removal scenarios. The largest tensile strains are found to be around 0.02 and the value is independent of the location
325 of the removed top chord members. It is noted that for commonly used structural steel a uniaxial tensile strain of 0.02 is
326 still in an early stage of material hardening and is far from tensile fracture. Therefore, the catenary action developed in the
327 bottom chord is normally sufficient to prevent progressive collapse, and it is a logical choice to take the deflection limit as
328 the failure criteria of the catenary action.

329 *Arch action*

330 According to the previous analysis, arch action provides the bridging-over capacity when a bottom chord member is
331 initially damaged. Because the undamaged sub-structures on both sides of the local failure are comprised of stable
332 triangular grids, they have excellent compressive strength and stiffness to support the formation of a strong arch action to
333 maintain the global stability. Failure to form a sufficient arch action is usually resulted from the buckling of individual

334 members inside the sub-structures. Taking the FE model of truss-PJ for example, as shown in Fig. 20, if the applied point
335 loads are doubled, the arch action will no longer remain stable upon the removal of BC3, and as a result progressive collapse
336 is triggered. This is initially caused by the buckling of the diagonal members next to the truss supports, i.e. DM1 and DM10.

337 Fig. 21 presents a simplified analytical model that reflects the arch action in a Warren truss subjected to a bottom-chord
338 member loss. Upon the formation of the arch action, the diagonal and bottom chord members adjacent to the truss supports,
339 i.e. the ‘edge diagonal member’ and ‘edge bottom chord member’, or DM1 and BC1 in truss-PJ, are subjected to the largest
340 compressive force as the external load is transferred eventually through these members to the truss supports. Consequently,
341 these members tend to experience earlier buckling than other compressive members. Based on the force equilibrium
342 condition, the compressive forces in DM1 and BC1 can be calculated by Eq. 5 and Eq. 6, and these equations show that
343 the compressive force in DM1 (N_{DM1}) is only determined by the distributed external load q and the angle between DM1
344 and BC1 γ , while the compressive force in BC1 (N_{BC1}) depends heavily on the local damage location (represented by the
345 local damage location parameter p), in addition to q and γ .

$$346 \quad N_{DM1} = \frac{qL}{2} \cdot \frac{1}{\sin \gamma} \quad (5)$$

$$347 \quad N_{BC1} = \frac{qL}{2} \left(\frac{p(1-p)}{H/L} - \cot \gamma \right) \quad (6)$$

348 where, H is the height of the truss, L is the truss span.

349 The previous FE analysis example shows first buckling of DM1 for the specific truss-PJ. But earlier buckling of BC1
350 (before that of DM1) could also occur when p is changed. In order to investigate which member buckles first under different
351 member removal conditions, a parameter named Buckling Index ($B.I.$) is introduced here. This index is defined as the ratio
352 of the compressive force of a member to its elastic buckling strength N_E , expressed in Eq. 7. If the buckling index of BC1
353 is larger than that of DM1, i.e. $B.I._{BC1}/B.I._{DM1} > 1$ (the ratio $B.I._{BC1}/B.I._{DM1}$ is calculated according to Eq. 8), BC1 buckles
354 first; otherwise, DM1 buckles first.

$$355 \quad B.I. = \frac{N}{N_E} \quad (7)$$

$$356 \quad \frac{B.I._{BC1}}{B.I._{DM1}} = \frac{N_{BC1} I_{BC1}^2 I_{DM1}}{N_{DM1} I_{DM1}^2 I_{BC1}} \quad (8)$$

$$= 4 \left(\frac{p(1-p)}{H/L} \cdot \sin \gamma - \cos \gamma \right) \cos^2 \gamma \cdot \frac{I_{DM1}}{I_{BC1}}$$

357 where, I_{BC1} and I_{DM1} is the moment of inertia of BC1 and DM1, respectively.

358 Fig. 22 presents the dependence of $B.I._{BC1}/B.I._{DM1}$ on p and the height-to-span ratio H/L ; the geometrical properties are
 359 taken as the same as truss-PJ, i.e. $\gamma=48^\circ$, $I_{BC1}/I_{DM1}=3.11$. For a truss with relatively large H/L ratio, such as truss-PJ with
 360 $H/L=0.113$, $B.I._{BC1}/B.I._{DM1}$ is always less than 1, indicating that DM1 always buckles first in this truss regardless of the
 361 location of initial damage (see Fig. 20). According to Eq. 5, N_{DM1} is independent of p , hence, the load resistance provided
 362 by the arch action q_{DM1} is also unrelated to the local damage location. For a truss with relatively small H/L ratio, such as
 363 truss-PJ-LS with $H/L=0.056$, local damage near the support ($p=0.1$ and 0.2) would still cause an earlier buckling of DM1,
 364 and the corresponding load resistance q_{DM1} is the same. q_{DM1} is also the threshold value for the loss of a bottom chord
 365 member near the mid-span to cause the buckling of DM1. However, when the local damage occurs near the mid-span of
 366 the truss, $B.I._{BC1}/B.I._{DM1}$ becomes larger than 1, indicating earlier buckling of BC1. In this case, the load resistance provided
 367 by the arch action q_{BC1} must be small than q_{DM1} , otherwise, DM1 shall buckle first. Therefore, for a truss with a small H/L
 368 ratio, smaller load resistance is provided by arch action when subjected to initial damage near the middle bottom chord
 369 member, i.e. the middle bottom chord member is the critical member.

370 FE analysis is performed to check the above propositions. As shown in Fig. 23, when a middle bottom chord member
 371 is removed from truss-PJ-LS, arch action fails due to the buckling of an edge bottom chord member, which is different
 372 from the FE analysis example shown in Fig. 20. The buckled edge bottom chord member is re-straightened during the
 373 downward deflection of the sub-structure. It is observed that, although the two edge bottom chord members are under
 374 identical compressive force according to Eq. 6 and the bilateral symmetric characteristic of the truss, the right-hand side
 375 member buckles first. This is because Eq. 6 has been proposed under the assumption that the remaining structure could

376 keep its exact original configuration when arch action develops; but due to the difference of the stiffness of the two sub-
377 structures, the “connection” that links the two sub-structures tends to move towards the one with longer span, and thus the
378 edge bottom chord member which is far from the local damage undergoes a slightly larger compressive force. When truss-
379 PJ-LS is subjected to a bottom-chord member loss close to the truss support, as shown in Fig. 24a, the arch action does not
380 fail, indicating that higher load resistance can be achieved by the arch action when a bottom chord member near the truss
381 support is initially damaged. This is consistent with the above conclusion of the critical members.

382 According to Fig. 22, for truss-PJ-LS subjected to the loss of a bottom chord member near the truss support, the failure
383 of the arch action, if it does develop, would be induced by the buckling of an edge diagonal member. To check this
384 prediction, the external load on truss-PJ-LS is doubled. As shown in Fig. 24b, the first buckled member is indeed the right
385 edge diagonal member. This phenomenon that buckling occurs in a side diagonal member far away from the local damage
386 can be explained by the same reason as previously stated which is not repeated here.

387 It is worth mentioning that the above discussion has been based on the assumption that the global stability of the sub-
388 structures on both sides of the local damage is secured. However this may not always be the case. As shown in Fig. 25,
389 when the side bottom chord member BC1 is removed, the left sub-structure reduces to a compressive slender member only
390 rather than any stable grids, and such a sub-structure can buckle easily under the dynamic impact caused by the sudden
391 removal of BC1. Clearly, it is very dangerous when a truss is subjected to the sudden loss of a side bottom chord. Therefore,
392 when the main collapse resistance is derived from the arch action, the critical members should include the edge bottom
393 chord members, as well as the bottom chord members in the mid-span.

394 **Conclusions**

395 Finite element and simplified analytical studies have been conducted on planar trusses subjected to local damage at different
396 locations. Two collapse-resisting mechanisms have been identified, namely, the catenary action and the arch action. The
397 development processes of these two mechanisms and the influencing factors have been investigated in detail. The following

398 conclusions can be drawn:

399 (1) When the initial local failure occurs to a top chord member, the bridging-over capacity of the remaining structure
400 is provided by the catenary action in the bottom chord; removal of the top chord member in the mid-span causes the most
401 severe damage to the overall structure.

402 (2) When the initial local failure occurs to a bottom chord member, the bridging-over capacity of the remaining structure
403 is provided by the arch action; removal of an edge bottom chord member and the bottom chord member in the mid-span
404 causes the most severe damage to the overall structure.

405 (3) When the initial local failure occurs to a diagonal member, there are two potential alternate load-transferring paths,
406 involving the arch action and the catenary action, respectively. The path involving an arch action in this scenario is normally
407 unstable, thus effectively the bridging-over capacity is mainly provided by the catenary action. Removal of the diagonal
408 member in the mid-span causes the most severe damage to the overall structure.

409 (4) Truss structures with vertical members are shown to have similar collapse-resisting mechanisms and critical
410 members as the truss structures without vertical members.

411 It should be noted that in the benchmark experimental program considered in this paper, pinned truss supports with no
412 horizontal degree of freedom were adopted, and this support condition has been followed in the numerical and analytical
413 studies in this paper. Because both the catenary action and the arch action generates considerable horizontal reaction force
414 at the supports, the horizontal strength and stiffness of the truss supports is expected to have significant influences on the
415 development of these two collapse-resisting mechanisms and hence the collapse resistance capacity. Different behavior
416 may be anticipated if the horizontal restraining conditions are changed. Generally speaking, for truss structures designed
417 with progressive collapse resistance, a sufficient horizontal strength and stiffness of the truss supports should be guaranteed.
418 The minimum requirements in this respect are to be studied in the follow-up research.

419 **Acknowledgement**

420 The work presented in this paper was funded by the National Natural Science Foundation of China (No. 51178332) and
421 the Foundation of State Key Laboratory of Disaster Reduction in Civil Engineering (No. sLDRCEO93-03). Technical input
422 from previous studies conducted by several PhD students in this research group, in particular Xiao-feng Jiang, Lei Wang,
423 is also gratefully acknowledged.

Reference

424

425 ABAQUS Inc. (2010). *ABAQUS Release 6.10 Documentation*. Providence, RI.

426 Astaneh-Asl, A. (2008). "Progressive Collapse of Steel Truss Bridges, the Case of I-35W Collapse." *Proceedings, 7th*
427 *International Conference on Steel Bridges*, Guimaraes, Portugal, 1-10.

428 Chen, J., Huang, X., Ma, R., et al. (2011). "Experimental study on the progressive collapse resistance of a two-story steel
429 moment frame." *Journal of Performance of Constructed Facilities*, 26(5), 567-575.

430 DoD (Department of Defense). (2009). "Design of buildings to resist progressive collapse." *Unified Facilities Criteria*
431 (UFC) 4-023-03, Washington, DC.

432 Fang, C., Izzuddin, B. A., Elghazouli, A. Y., et al. (2011). "Robustness of steel-composite building structures subject to
433 localised fire." *Fire Safety Journal*, 46(6), 348-363.

434 Fu, F. (2009). "Progressive collapse analysis of high-rise building with 3-D finite element modeling method." *Journal of*
435 *Constructional Steel Research*, 65(6), 1269-1278.

436 GSA (General Services Administration). (2003). "Progressive Collapse Analysis and Design Guidelines for New Federal
437 Office Buildings and Major Modernization Projects." Washington, DC.

438 Hallquist, J. O. (2007). *LS-DYNA keyword user's manual, Version 971*. Livermore, CA.

439 Izzuddin, B. A. (2005). "A simplified model for axially restrained beams subject to extreme loading." *International Journal*
440 *of Steel Structures*, 5(5), 421-429.

441 Jiang, X., and Chen, Y. (2012). "Progressive Collapse Analysis and Safety Assessment Method for Steel Truss Roof."
442 *Journal Performance of Constructed Facilities*, 26(3), 230-240.

443 Khandelwal, K., El-Tawil, S., Sadek, F. (2009). "Progressive collapse analysis of seismically designed steel braced frames."
444 *Journal of Constructional Steel Research*, 65(3), 699-708.

445 Levy, M., and Galvadori, M. (1992). *Why Buildings Fall Down - How Structures Fail*, New York, NY: W.W. Norton &

446 Company.

447 Luccioni, B. M., Ambrosini, R. D., Danesi, R. F. (2004). "Analysis of building collapse under blast loads." *Engineering*

448 *Structures*, 26(1), 63-71.

449 Malla, R. B., and Nalluri, B. B. (2000). "Dynamic nonlinear member failure propagation in truss structures." *Structural*

450 *Engineering and Mechanics*, 9(2), 111-126.

451 Marjanishvili, S. M. (2004). "Progressive analysis procedure for progressive collapse." *Journal of Performance of*

452 *Constructed Facilities*, 18(2), 79–85.

453 Marjanishvili, S. M., and Agnew, E. (2006). "Comparison of various procedures for progressive collapse analysis." *Journal*

454 *of Performance of Constructed Facilities*, 20(4), 365–74.

455 Miyachi, K., Nakamura, S. and Manda, A. (2012). "Progressive collapse analysis of steel truss bridges and evaluation of

456 ductility." *Journal of Constructional Steel Research*, 78, 192-200.

457 Murtha-Smith, E. (1988). "Alternate path analysis of space trusses for progressive collapse." *Journal of Structural*

458 *Engineering - ASCE*, 114(9), 1978-1999.

459 NIST (National Institute of Standards and Technology). (2005). "The collapse of the World Trade Center towers." NIST

460 NCSTAR 1, Gaithersburg, MD.

461 NTSB (National Transportation Safety Board). (2008). "Highway Accident Report, Collapse of I-35W Highway Bridge,

462 Minneapolis, Minnesota August 1, 2007." NTSB/HAR-08/03PB 2008–916203.

463 Powell, G. (2005). "Progressive collapse: case study using nonlinear analysis." *ASCE Structures Congress and Forensic*

464 *Engineering Symposium*, New York, 1-14.

465 Sasani, M., and Kropelnicki, J. (2008). "Progressive collapse analysis of an RC structure." *The Structural Design of Tall*

466 *and Special Buildings*, 17(4), 757-771.

467 Sasani, M., and Sagiroglu, S. (2008). "Progressive collapse resistance of Hotel San Diego." *Journal of Structural*

468 Engineering - ASCE, 134(3), 478-488.

469 Smith, E.A., and Epstein, H. I. (1980). "Hartford coliseum roof collapse: structural collapse sequence and lessons learned."
470 Civil Engineering - ASCE, 50(4), 59-62.

471 Song, B.I., Giriunas, K. A., Sezen, H. (2014). "Progressive collapse testing and analysis of a steel frame building." Journal
472 of Constructional Steel Research, 94, 76-83.






473 Tsai, M.H., and Lin, B. H. (2008). "Investigation of progressive collapse resistance and inelastic response for an
474 earthquake-resistant RC building subjected to column failure." Engineering Structures, 30(12): 3619-3628.

475 Wang, L. (2010). "Study on test and numerical simulation of progressive collapse for truss/beam-type structural systems."
476 (Doctoral Thesis) Shanghai: Tongji University. (in Chinese)

477 Yi, W., He, Q., Xiao, Y., et al. (2008). "Experimental study on progressive collapse-resistant behavior of reinforced concrete
478 frame structures." ACI Structural Journal, 105(4), 433-439.

479 Zhao, X., Yan, S., Chen, Y., et al. (2016). "Experimental study on progressive collapse-resistant behavior of planar trusses."
480 Engineering Structures. (under review)

Table 1. Comparison of test and FE results of truss-RJ.

Event	Time (s)		Deformation (obtained by FE analysis)
	Test	FEM	
Intact	0.00	0.00	
Bottom end of DM3 yields	0.18	0.17	
DM3 buckles	0.41	0.37	
DM5 buckles	0.67	0.67	
DM4 buckles	0.87	0.88	
TJ2 drops onto bottom chord	1.19	1.38	